Analytica Chimica Acta 699 (2011) 206–215

Contents lists available at ScienceDirect

Analytica Chimica Acta

journal homepage: www.elsevier.com/locate/aca

Multi-step surface functionalization of polyimide based evanescent wave photonic biosensors and application for DNA hybridization by Mach-Zehnder interferometer

Eva Melnik[a,b], Roman Bruck[a], Rainer Hainberger[a,*], Michael Lämmerhofer[b,**]

[a] Health & Environment Department, Nano Systems, AIT Austrian Institute of Technology GmbH, Donau-City-Straße 1, 1220 Vienna, Austria
[b] Department of Analytical Chemistry, University of Vienna, Waehringer Strasse 38, 1090 Vienna, Austria

ARTICLE INFO

Article history:
Received 29 March 2011
Received in revised form 10 May 2011
Accepted 11 May 2011
Available online 20 May 2011

Keywords:
Polyimide spin-coated silicon wafer
Surface modification
Biosensor
Biotin–streptavidin DNA hybridization
Mach-Zehnder interferometer

ABSTRACT

The process of surface functionalization involving silanization, biotinylation and streptavidin bonding as platform for biospecific ligand immobilization was optimized for thin film polyimide spin-coated silicon wafers, of which the polyimide film serves as a wave guiding layer in evanescent wave photonic biosensors. This type of optical sensors make great demands on the materials involved as well as on the layer properties, such as the optical quality, the layer thickness and the surface roughness. In this work we realized the binding of a 3-mercaptopropyl trimethoxysilane on an oxygen plasma activated polyimide surface followed by subsequent derivatization of the reactive thiol groups with maleimide-PEG_2-biotin and immobilization of streptavidin. The progress of the functionalization was monitored by using different fluorescence labels for optimization of the chemical derivatization steps. Further, X-ray photoelectron spectroscopy and atomic force microscopy were utilized for the characterization of the modified surface. These established analytical methods allowed to derive information like chemical composition of the surface, surface coverage with immobilized streptavidin, as well as parameters of the surface roughness. The proposed functionalization protocol furnished a surface density of 144 fmol mm^{-2} streptavidin with good reproducibility (13.9% RSD, $n = 10$) and without inflicted damage to the surface. This surface modification was applied to polyimide based Mach-Zehnder interferometer sensors to realize a real-time measurement of streptavidin binding validating the functionality of the MZI biosensor. Subsequently, this streptavidin surface was employed to immobilize biotinylated single-stranded DNA and utilized for monitoring of selective DNA hybridization. These proved the usability of polyimide based evanescent photonic devices for biosensing application.

1. Introduction

The need for rapid and selective online analysis of biological components in industry and medicine is almost infinite. Optical biosensors promise to fulfil the main requirements for fast, sensitive, low cost and selective multiparameter analysis on robust and small devices. In particular, evanescent wave biosensors allow a highly sensitive label-free real-time detection of biomolecular interactions. They have been implemented as ring resonators [1], grating based devices [2] or Mach-Zehnder interferometers [3] and successfully applied in medical diagnostics [4], fundamental research [5] and environmental monitoring [6,7]. Evanescent wave sensors comprise a thin optical waveguide layer, the refractive index and thickness of which determine the surface sensitivity [8,9] of the sensor. Most sensors demonstrated so far employed inorganic waveguide materials such as silicon [10] or silicon nitride [11]. For these materials, the surface functionalization chemistry is well-established.

Polymers, on the other hand, also represent an attractive material system as substrate for building optical waveguide sensors because they allow for cost-effective fabrication techniques such as spin coating, hot embossing and injection molding. The disadvantage of polymers in general is the limited range of refractive indices that lead to a lower surface sensitivity compared to inorganic materials. Critical issues for the choice of a suitable waveguide polymer for evanescent wave sensors are a good transparency at the desired wavelength, a high refractive index, and a high chemical resistivity. Moreover, it should allow for thicknesses well below 1 μm. Polyimide (PI) fulfils all these requirements. [1,2,34].

* Corresponding author. Tel.: +43 050550 4304; fax: +43 050550 4399.
** Corresponding author at: University of Vienna, Faculty of Chemistry, Department of Analytical Chemistry, Waehringer Strasse 38, A-1090 Vienna, Austria. Tel.: +43 1 4277 523 23; fax: +43 1 4277 9523.
E-mail addresses: rainer.hainberger@ait.ac.at (R. Hainberger), michael.laemmerhofer@univie.ac.at (M. Lämmerhofer).

0003-2670/$ – see front matter © 2011 Elsevier B.V. All rights reserved.
doi:10.1016/j.aca.2011.05.017

However, since there have been only few demonstrations of polyimide based biosensors, there are rarely any optimized functionalization protocols available, in particular none that is fully compatible with the requirements given by the optical sensor concept.

In this paper, we report the optimization of the surface modification of polyimide films used as waveguiding layer in evanescent wave sensors. A successful protocol for the chemical functionalization is proposed employing the biotin–streptavidin biorecognition principle as model system [13] and subsequently for immobilization of biotinylated ligands such as single-stranded DNA.

For surface modifications of polyimide films some literature exists, describing protocols such as photoreactions [14], aminolytic ring opening reactions [15] that have been utilized for the functionalization with cyclodextrins [16], and alkaline hydrolysis [17–19]. The chemical route of alkaline hydrolysis leads to surface amides and carboxylic acids. Subsequent reactions of resultant carboxylic acids may be performed with various reagents such as hydrazines, epoxides, amines, alcohols and aminosilanes [20]. Also the derivatization of the surface carboxylic groups by activation with *N*-(3-dimethylaminopropyl)-*N*-ethylcarbodiimide (EDC) followed by reaction with diamine is well known [21]. However, we observed that alkaline hydrolysis and functionalization in hot solvents severely damage thin polyimide layers and, therefore, cannot be used for our purpose.

For our application, we have to ensure that the approximately 400 nm thin polyimide film does not get thinned or damaged and that the surface roughness stays at an acceptable degree.

In contrast to commonly used methods such as alkaline hydrolysis we chose oxygen plasma to form reactive oxygen species on the polyimide surface. The effects of atomic oxygen [22], oxygen plasma exposure [23] and oxygen reactive ion etching (RIE) [24] on polyimide surfaces are well described. Judging from these reports we were expecting that the oxygen plasma exposure does not destroy our thin film of polyimide, but leads to surface peroxides [24] and hydroxyl groups [25] after dipping the activated surface into water. These reactive groups can serve as binding sites in the first functionalization step with 3-mercaptopropyl trimethoxysilane (MPTMS), which carries reactive thiol groups and subsequently may react specifically with the maleimide moiety of maleimide-PEG_2-biotin. The resulting biotinylated polyimide surface is used to immobilize streptavidin. The interaction between biotin and streptavidin is commonly used to validate the sensitivity of biosensors [26–28] because of the high mass of streptavidin (60 kDa) that serves as analyte and the strong affinity between biotin and streptavidin (binding constant $K_a \approx 10^{14}\,L\,mol^{-1}$).

In order to monitor the success of the surface reactions, various analytical methods have been used. On the one hand, the optimization of the surface reactions has been performed employing two different fluorescence labelled molecules, namely tetramethyl rhodamine-5-maleimide (TMR5M) and Chromeon 642-streptavidin. On the other hand, after each step of functionalization reaction i.e. before and after oxygen plasma exposure, after silanization with MPTMS, derivatization with maleimide-PEG_2-biotin, and binding of streptavidin the surface was analyzed by means of X-ray photoelectron spectroscopy (XPS) which provided valuable information on the success of the respective chemical reactions. Atomic force microscopy (AFM) yielded additional information about the surface roughness at each level of modification.

The established surface modification protocol enables the real-time measurements of streptavidin on polyimide based Mach-Zehnder interferometer (MZI) sensors and builds a platform for selective DNA hybridization experiments. These measurements proved the usability of polyimide based evanescent photonic devices for biosensing applications.

2. Experimental

2.1. Control samples and polyimide based MZI sensors

The control samples consisted of polyimide (PI) films made from Pyralin® PI-2771 (purchased form HD Microsystems, Neu-Isenburg, Germany), which is a copolyimide obtained from benzophenone tetracarboxylic dianhydride (BTDA) and the two types of diamine p,p′-oxydianiline (ODA) and m-phenylenediamine. The PI films were spin-coated on crystalline silicon wafers covered with 5 μm silicon oxide. The spun films were soft baked at 100 °C (1 min), exposed to UV light at 365 nm (30 s) and finally hard baked at 200 °C (1 h). On these control polyimide samples the surface modification was optimized. The Mach-Zehnder interferometer (MZI) sensors used for biosensing were produced by conventional lithographic and reactive ion etching steps of silicon dioxide covered crystal silicon. After etching of the waveguide structure the polyimide film was processed as described for the control samples. For the last step of the MZI sensor fabrication, an inorganic–organic hybrid polymer cladding (Ormoclad from Microresist technology GmbH, Berlin, Germany) was spin-coated on the sensor surface, soft baked at 100 °C (2 min), exposed to UV light at 365 nm (90 s), post baked at 120 °C (5 min) and finally hard baked at 150 °C (180 °C).

2.2. Materials

3-Mercaptopropyl trimethoxysilane (MPTMS), triphenyl phosphine, 4-dimethylaminopyridine (DMAP), tetramethylrhodamine-5-maleimide (TMR5M), bovine serum albumin (BSA), Chromeon 642-labelled streptavidin and unlabelled streptavidin from *Streptomyces avidinii* were purchased from Sigma Aldrich, Vienna, Austria. Maleimide-PEG_2-biotin (M-PEG_2-biotin) was supplied by Fischer Scientific, Vienna, Austria. The 25-nucleotide biotin-tagged ssDNA (biotin-ssDNA; 5′-TCG CCA TTC GTT GAC TAC TTC TTA T-3′-biotin) and its complementary Cy5-labelled ssDNA (3′-AGC GGT AAG CAA CTG ATG AAG AAT A-5′-Cy5) as well as non-complementary Cy3-labelled ssDNA (3′-TTG CTC TGA GGC AGA GTT T-5′-Cy3) was purchased from VBC Biotech GmbH, Campus Vienna, Austria.

The non-complementary and complementary ssDNA were labelled with Cy3 and Cy5 fluorescence markers, which offers the possibility for a control fluorescence scan.

2.3. Surface chemistry

2.3.1. Activation of the surface

For cleaning and activation the polyimide control samples were treated with oxygen plasma, at room temperature, 40 W power and 1 mbar with plasma system Femto (generator: 2.45 GHz) from Diener, Stuttgart, Germany. The treatment time was optimized between 10 s and 5 min.

2.3.2. Silanization of polyimide surface

For the silanization the activated polyimide control samples were dipped in different MPTMS solutions for 1 h at room temperature. Thus, different MPTMS solutions were tested: First, MPTMS (3%, v/v) in toluene with basic catalyst DMAP (3%, w/v). Second, acidic aqueous MPTMS solution composed of (3%, v/v) MPTMS in 0.07 M acetate buffer pH 5.5, 2.8% (v/v) TritonX-100, and 25% (v/v) methanol. Subsequently, the reaction time of the best solution was optimized between 30 min and 2 h. After the silanization the samples were cleaned in the ultrasonic bath in isopropyl alcohol for 5 min, then washed with ultrapure water and again isopropyl alcohol, and dried under nitrogen stream.

2.3.3. Labeling with TMR5M and biotinylation

For labeling with TMR5M the silanized polyimide control samples were spotted via pipette with different concentrations of TMR5M in ultrapure water with 10% (v/v) isopropanol and 10% (v/v) phosphate buffer 0.05 M pH 7.0.

For the biotinylation the silanized polyimide samples were dipped in 5 μM M-PEG_2-biotin dissolved in ultrapure water with 10% (v/v) isopropanol and 10% (v/v) phosphate buffer 0.05 M pH 7.0.

After the labeling with TMR5M or biotinylation the samples were cleaned two times with ultrapure water and one time with isopropyl alcohol and dried under nitrogen stream.

2.3.4. Immobilization of Chromeon 642-streptavidin

For the immobilization of Chromeon 642-streptavidin biotinylated control samples were spotted via pipette with 1 μM Chromeon 642-streptavidin. After a reaction time of 1 h the samples were cleaned two times with ultrapure water and dried under nitrogen stream.

2.3.5. Blocking tests with BSA

The blocking of the silanized (reference sample) and the biotinylated polyimide control samples were realized by shaking in 100 μg mL^{-1} BSA dissolved in 150 mM PBS buffer for 30 min. After blocking with BSA, the samples were cleaned two times with ultrapure water and dried under nitrogen stream. The BSA blocked samples were spotted with 1 μM Chromeon 642-streptavidin. After a reaction time of 1 h the control samples were cleaned two times with ultrapure water and dried under nitrogen stream.

Via measurement of the fluorescence intensity of the Chromeon 642-streptavidin of blocked and unblocked samples specific and unspecific binding of streptavidin to the surfaces was determined.

2.3.6. Optimized surface modification protocol

The resulting optimized procedure was as follows: 1 min oxygen plasma activation, silanization in acidic aqueous MPTMS solution for 1 h, biotinylation with 5 μM M-PEG_2-biotin for 1 h. This procedure was used to functionalize the polyimide based MZI sensors with biotin.

2.4. Methods

2.4.1. Contact angle measurement

The water contact angle was measured at room temperature by spotting via pipette 5 μL ultrapure water on the untreated and the oxygen plasma activated polyimide surfaces. Contact angles were determined by drop shape analysis and every sample was analyzed two times.

2.4.2. Fluorescence scan

Fluorescence scans were performed with the ArrayPro® TECAN fluorescence scanner from Media Cybernetics in Bethesda, USA with 633 nm or 532 nm excitation wavelength and 692 nm or 575 nm emission filter for Chromeon 642 and TMR5M, respectively.

2.4.3. Characterization with AFM

The Pico Plus atomic force microscope (AFM) from Molecular Imaging, Tempe, USA, was used to analyze the polyimide samples after each step of the optimized functionalization protocol. Therefore, the measurements were done in tapping mode, under air, with small measurement area (1 μm^2), using NANOSENSORS™ AFM tips, Type: PPP-NCHR-50 (4.0 ± 1 μm wide, 125 ± 10 μm length, tip radius < 10 nm).

2.4.4. Characterization with XPS

X-ray photoelectron spectra (XPS) were measured before and after the various steps of the optimized functionalization protocol with the Phoibos-Hsa3500 instrument from SPECS Surface Nano Analysis GmbH, Berlin, Germany, using Magnesium X-ray source with 1253 eV emission line and 30° measurement angle. The individual atom peaks from the XPS spectra were deconvoluted by use of the deconvolution software of CasaXPS Version 2.3.15. in order to derive information on the bonding status of the atoms.

2.4.5. Measurements with the polyimide based evanescent wave MZI biosensors

An evanescent wave Mach-Zehnder Interferometer (MZI) was used as sensing element of the polyimide-based biosensor. A tunable laser with a central wavelength of 1310 nm acts as light source for the MZI and the coupling of light to the polymer waveguides was done by end-face coupling from optical fibers. In our MZI, the propagating mode from the input waveguide gets split into a measurement and reference arm by means of a Y-junction and after a distance of 10 mm the light from these two arms is recombined again by another Y-junction.

The reference arm of the MZI is covered with a cladding layer (Ormoclad), so that binding events on the sensor surface can only influence the propagation of the waveguide mode in the measurement arm, which subsequently leads to a sinusoidal modulation of the output signal as function of the effective index of the measurement arm at the end of the interferometer. During a measurement, the intensity is recorded as function of time and the accumulated phase shift was calculated by reversing the sinusoidal characteristic of the MZI.

On top of the sensor a PDMS fluidic chamber was mounted, in which the sample fluids were carried over the surface by an electronically controlled host-syringe pump system. A detailed description of the measurement setup can be found elsewhere [12].

Measurements of Chromeon 642-streptavidin binding, the monitoring of the immobilization of the unlabelled streptavidin and ssDNA hybridization experiments were performed.

3. Results and discussion

In this section first a detailed description on the optimization of the employed surface modification protocol is given. The multiple steps of functionalization of the polyimide surface consist of activation (by oxygen plasma exposure), silanization, labeling with TMR5M and biotinylation, and finally immobilization of streptavidin, each of which will be outlined below in more detail. After optimization real-time measurements with the polyimide based MZI sensors will be described to document the functionality of surface chemistry and sensor device.

3.1. Activation

The polyimide surface is chemically relatively inert and hydrophobic. Hence, for efficient chemical derivatization by silanization it was deemed necessary to perform an activation step in order to introduce appropriate chemical groups for reaction with silanes and make the surface more hydrophilic to promote adhesion. This activation of the polyimide surface was realized using oxygen plasma exposure. For this purpose, the polyimide samples were transferred into the Femto plasma system and treated for different times (0, 10, 30 s and 1, 3, 5 min). Contact angle measurements of the polyimide samples with a water drop have shown that the contact angle varies from 83° before the treatment, to 3° after 3 min oxygen plasma treatment, while it cannot be further reduced using longer treatment times. The decrease of the contact angle

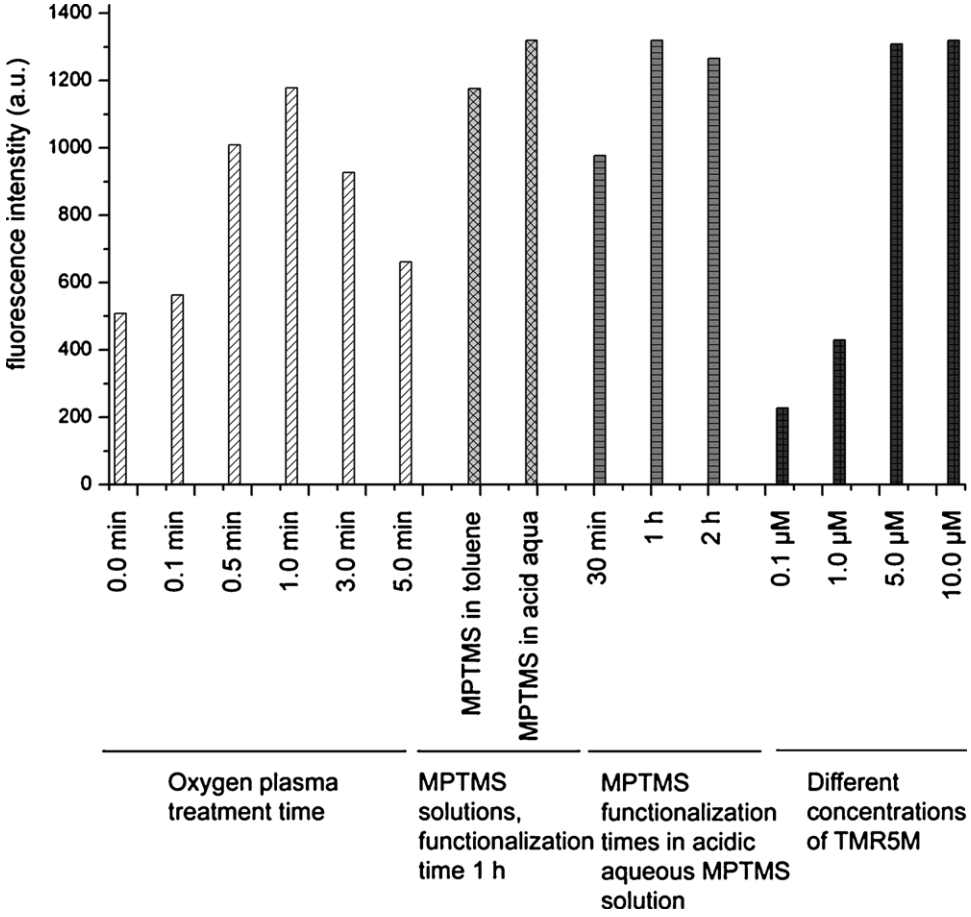

Fig. 1. Overview of the most important parameters, which were optimized via fluorescence scan. The fluorescence intensity of the label TMR5M was measured at 532 nm excitation wavelength and 575 nm emission filter with a fluorescence scanner.

indicates the introduction of polar oxygen species which make the surface more hydrophilic.

For monitoring and optimizing the effect of different activation times in terms of silanization degree, the oxygen plasma activated samples were dipped in acidic aqueous MPTMS solution for 1 h and then labelled with 10 μM TMR5M for 1 h. The fluorescence intensities of the different samples were measured at 532 nm excitation wavelength and 575 nm emission filter with a fluorescence scanner. With increase of oxygen plasma treatment time, the fluorescence intensity could be enhanced. This trend can be attributed to the introduction of a higher density of reactive oxygen species which allows a more efficient derivatization with MPTMS and enables the formation of a denser silane layer that is accompanied by a higher surface coverage with thiols. The highest fluorescence intensity was reached at 1 min oxygen plasma treatment time (see Fig. 1). At higher treatment times (3 and 5 min) the fluorescence intensity decreased. This effect may indicate the onset of etching processes of the polyimide leading to erosion of the polyimide film [22].

3.2. Silanization of polyimide surface

A more hydrophilic surface with increased oxygen concentrations, some of which may react with alkoxysilanes by condensation forming stable C–O–Si bonds between polyimide and MPTMS, is supposed to be favorable for the following silanization step. In any case, it favors the adhesion of the silane layer. The silanization yield on the activated polyimide surface was first tested with two distinct 3% (v/v) MPTMS solutions, namely MPTMS in toluene with basic catalyst DMAP and acidic aqueous MPTMS solution.

Therefore, the 1 min oxygen plasma activated samples were dipped in the MPTMS solutions for 1 h and afterwards the samples were labelled with 10 μM TMR5M for 1 h. The higher fluorescence intensity was reached for the acidic aqueous MPTMS solution, which was therefore adopted as the preferable silanization reagent. Under acidic aqueous conditions a polymeric silane bonding is most likely formed yielding higher surface concentrations of active sulfhydryls for the following step. In contrast, silanization in organic media and basic catalyst is known to provide a less dense brush-type bonding.

Next, the optimal reaction time for the silanization step was examined for the acidic aqueous MPTMS solution at 30 min, 1 h and 2 h. After 1 h reaction time the fluorescence intensity does not further increase, which indicates that the reaction is completed after 1 h (see Fig. 1).

3.3. Labeling with TMR5M and biotinylation

After silanization, the surface carries reactive sulfhydryl functional groups which can readily react with the maleimide moiety of the fluorescence label TMR5M used for monitoring of the extent of surface modification or of the M-PEG_2-biotin used as biorecognition ligand for streptavidin. Due to exposure to oxygen e.g. air dissolved in reaction solutions, a certain fraction of thiols might be inactivated by oxidation to disulfides. To re-activate such inert disulfides, phosphine reagents such as triphenyl phosphine or tris(2-carboxyethyl)phosphine can be used for reduction [29]. The effect of a triphenyl phosphine pre-treatment on the surface concentration of reactive thiols was tested by monitoring the fluo-

rescence intensity after labeling with TMR5M. It was found that this additional reduction step does not improve the resultant surface coverage with reactive thiols.

The reaction time for the maleimide coupling step was optimized with TMR5M and monitoring by UV spectrophotometry in solution at 300 nm via disappearance of absorption due to loss of conjugated double bond of the maleimide moiety as described in detail in the literature [30]. The optimal reaction time was found by measurement of the transmission at 300 nm at different times (0, 15, and 30 min as well as 1, and 2 h). After 1 h reaction time the transmission does not change anymore and the reaction is complete.

Furthermore, the optimal concentration of the maleimide reagent was determined by spotting, via a pipette, different concentrations of the label TMR5M on the surface and analyzing their fluorescence intensity after 1 h reaction time. Thereby, it was found that the fluorescence intensity increases up to a concentration of 5 μM TMR5M, while it stays constant at higher concentrations (see Fig. 1). With this information the concentration of M-PEG_2-biotin for functionalization was also fixed at 5 μM under the same conditions as the labeling with TMR5M.

3.4. Ligand immobilization

3.4.1. Immobilization of Chromeon 642-streptavidin

The final step of streptavidin binding to the surface was conveniently monitored and optimized by use of fluorescence-labelled streptavidin. Thus, 1 μM Chromeon 642-streptavidin in 150 mM PBS buffer was spotted via pipette on ten different biotinylated control samples. After a reaction time of 1 h and cleaning, the samples were analyzed by fluorescence scan. The fluorescence intensity was measured at 633 nm excitation wavelength and 692 nm emission filter with a fluorescence scanner.

For the quantification a calibration set was prepared on untreated polyimide samples. To do so, different concentrations (10–200 fmol mm^{-2}) of Chromeon 642-streptavidin were spotted on untreated polyimide samples and the spots were dried at room temperature in the dark to create a solid standard array. By use of the resulting calibration curve ($y = 19.71 \pm 0.83 \times -44.60 \pm 83.73$; $n = 5$, $r = 0.9973$) with a detection limit of 15.39 ± 0.4 fmol mm^{-2} a concentration of 144 ± 20 fmol mm^{-2} was determined for ten biotinylated samples. This result for the surface coverage with streptavidin is higher than what can be expected in theory on a perfectly planar surface. The streptavidin ligand has a size of 4.5 nm × 4.5 nm × 5.8 nm [31] and occupies a binding area of 26 nm^2. By optimal (100%) packing density the concentration of the streptavidin on the planar surface would be estimated as 64 fmol mm^{-2}. The published closest coverages of streptavidin on planar surfaces are about 66% (42 fmol mm^{-2}) for two dimensional crystals [31,32] and 40% (26 fmol mm^{-2}) [26] on a silicon surface with a streptavidin monolayer. Higher concentrations of streptavidin, e.g. 37,000 fmol mm^{-2} have been achieved employing a three-dimensional binding matrix [33]. Our result of 144 ± 20 fmol mm^{-2} evidently lies in-between these reported values.

3.4.2. BSA blocking to verify the specific and unspecific binding behavior

Both specific and unspecific binding can contribute to the concentration of 144 fmol mm^{-2} streptavidin on the surface in above binding experiments on the biotinylated polyimide surface. To deconvolute specific and unspecific binding contributions, streptavidin binding was determined on reference samples with silanized surface and biotinylated surface before and after blocking unspecific binding sites with BSA. No fluorescence of Chromeon 642-streptavidin could be detected on the prepared silanized reference samples after BSA blockade. In contrast, the unblocked samples showed an unspecific binding of 63 ± 25 fmol mm^{-2} of Chromeon 642-streptavidin to the polyimide surface. The BSA blocked biotinylated surface on the other hand showed after Chromeon 642-streptavidin immobilization a fluorescence intensity corresponding to approximately 80 ± 22 fmol mm^{-2} streptavidin on the biotinylated BSA blocked polyimide surface. This shows that the unspecific binding can be effectively suppressed by rinsing with BSA before streptavidin immobilization.

3.5. AFM analysis of the optimized modified surfaces

While a roughened surface might yield higher surface areas and consequently more ligands on the sensing layer, thickness and surface roughness are critical factors, as mentioned above, and have to be kept under careful control. For this reason, thickness and surface roughness were monitored by atomic force microscopy (AFM). Polyimide samples were analyzed by AFM in tapping mode before treatment, after MPTMS modification and biotin functionalization, as well as after streptavidin immobilization (see Fig. 2). The untreated polyimide film showed a smooth surface with a mean roughness, R_a, of 0.379 nm. After the MPTMS functionalization the surface roughness increased to a R_a of 0.56 nm and some nanoporous structures having nano-channels with a maximal depth of 10 nm and a diameter of up to 50 nm have been found. The surface behavior of the biotin functionalized sample was similar, with a R_a of 0.57 nm. After the immobilization of Chromeon 642-streptavidin the surface shows in comparison less nanoporous structures and the maximal depth was about 3 nm.

These results prove that the proposed polyimide film functionalization method does not cause a significant change of the surface roughness. The variations in the sub-nanometer range do not induce an appreciable propagation loss of the guided light, when the polyimide is used as waveguide layer in evanescent wave photonic biosensors.

3.6. XPS analysis of optimized functionalized surfaces

Surface chemical compositions as investigated by XPS can give valuable information on the progress and success of surface reactions. Thus, XPS spectra have been acquired for the untreated polyimide surface, after the oxygen plasma treatment, the MPTMS and biotin functionalization, as well as after the streptavidin immobilization, after each individual step has been optimized.

In Fig. 3 the XPS spectrum of the untreated polyimide surface is shown. The untreated PI surface shows the expected peaks of oxygen (531.21 eV), nitrogen (399.71 eV) and carbon (283.96 eV), according to the composition of the polyimide layer, but also the peaks of silicon (152.24 and 101.21 eV). The silicon peaks are caused by the silane additive in the Pyralin® PI-2771 start material. By deconvolution of the different atom peaks of the XPS spectra, information on the relative surface concentrations of the different bonding states of the atomic species and how they vary in the course of the surface modification process can be derived. In Fig. 5, a detailed overview of the main peaks of such deconvoluted spectra before and after the functionalization steps are given. The relative atom compositions of the surface at the distinct levels of modification as determined by integration from the atom peaks of the XPS spectra are summarized in Fig. 6.

The first step of the polyimide surface modification protocol, the oxygen plasma activation, increases the oxygen content on the surface, while the carbon peak decreases (Fig. 4). The analysis of the oxygen peaks in the XPS spectra shows that especially the concentration of carbonyl oxygen (C=O) and the peak of C–O species is increased. The concentration of carboxyl groups (O=C–OH) is

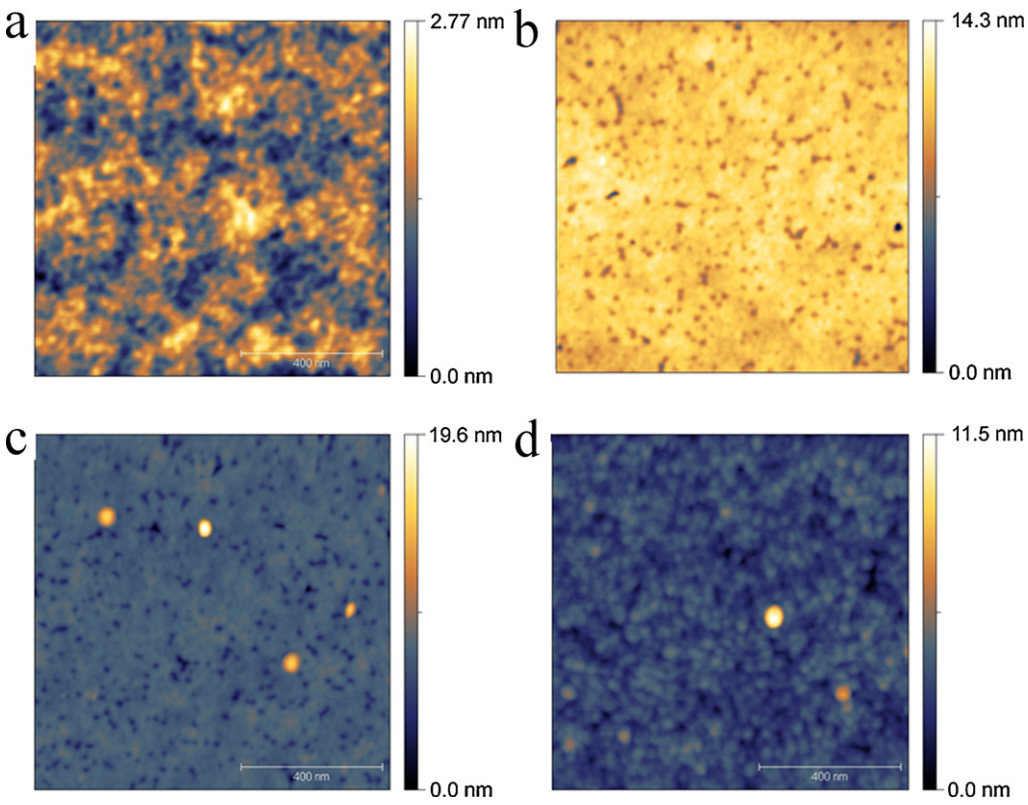

Fig. 2. AFM measurements of the polyimide surface for (a) the untreated surface, (b) the MPTMS functionalized surface, (c) the biotin functionalized surface and (d) the surface after immobilization of Chromeon 642-streptavidin.

reduced with the treatment, showing that the oxygen plasma is not useful to generate a reasonable number of carboxyl groups on the surface, which is an important difference to basic treatments [17–19]. In the literature it is suggested that the oxygen plasma causes first a formation of C–O species, such as peroxides, on the surface and finally leads to an etching process of the polyimide via the formation of carbon dioxide and monoxide gas [22]. From our results we may conclude that the oxygen plasma first forms a critical level of highly reactive oxygen species on the surface before a significant etching process starts. Via carefully timed oxygen plasma treatment and resultant increase of the reactive oxygen groups on the PI surface one should be able to regulate the MPTMS binding capacity. At a critical level of the oxygen concentration on the surface a significant etching process occurs. This leads to a decrease of adhesion and binding of MPTMS. Simultaneously, also the subsequent biotin ligand density is reduced leading to lower streptavidin concentrations as well (as discussed before, see Fig. 1). In the XPS spectra also a change of the nitrogen peak can be noticed upon plasma oxygen treatment. Close to the original amine ($-NH_2$) and amide (O=C–N) peak an additional peak of nitrogen oxides (N–O) can be found (Fig. 4). Further, the carbon C–<!– no-mfc –>C/C<!– /no-mfc –>–H peak is decreased while C=O and C–O are both increased. This is supposed to be favorable for the bonding and adhesion of the subsequent silane layer.

The next functionalization step is the dipping of the oxygen plasma activated polyimide films into the acidic aqueous MPTMS solution. As can be seen from Fig. 4, the relative intensity of the O1s peak is reduced while that of the C1s peak slightly enhanced, as expected. The resulting changes in the atom bonding states of the XPS spectra indicate a decrease of the carbonyl groups

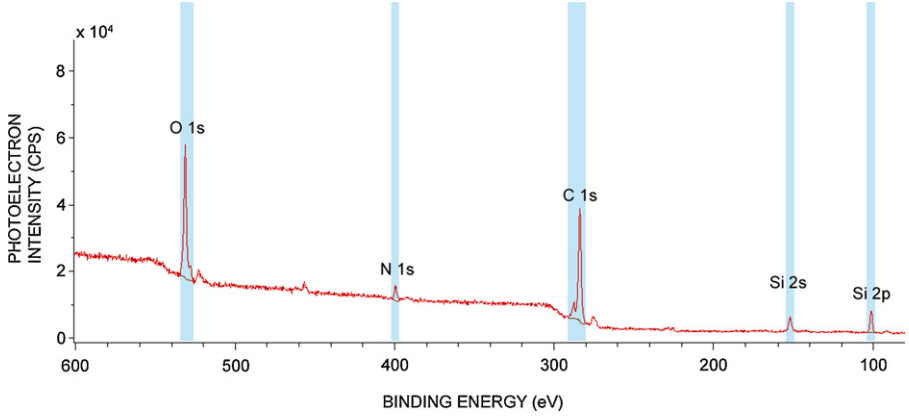

Fig. 3. X-ray photoelectron spectra (XPS) of the untreated polyimide surface. Peaks found for oxygen (531.21 eV), nitrogen (399.71 eV), carbon (283.96 eV) and silicon (152.24 and 101.21 eV). The silicon peaks are caused by the silane additive in the Pyralin® PI-2771 start material.

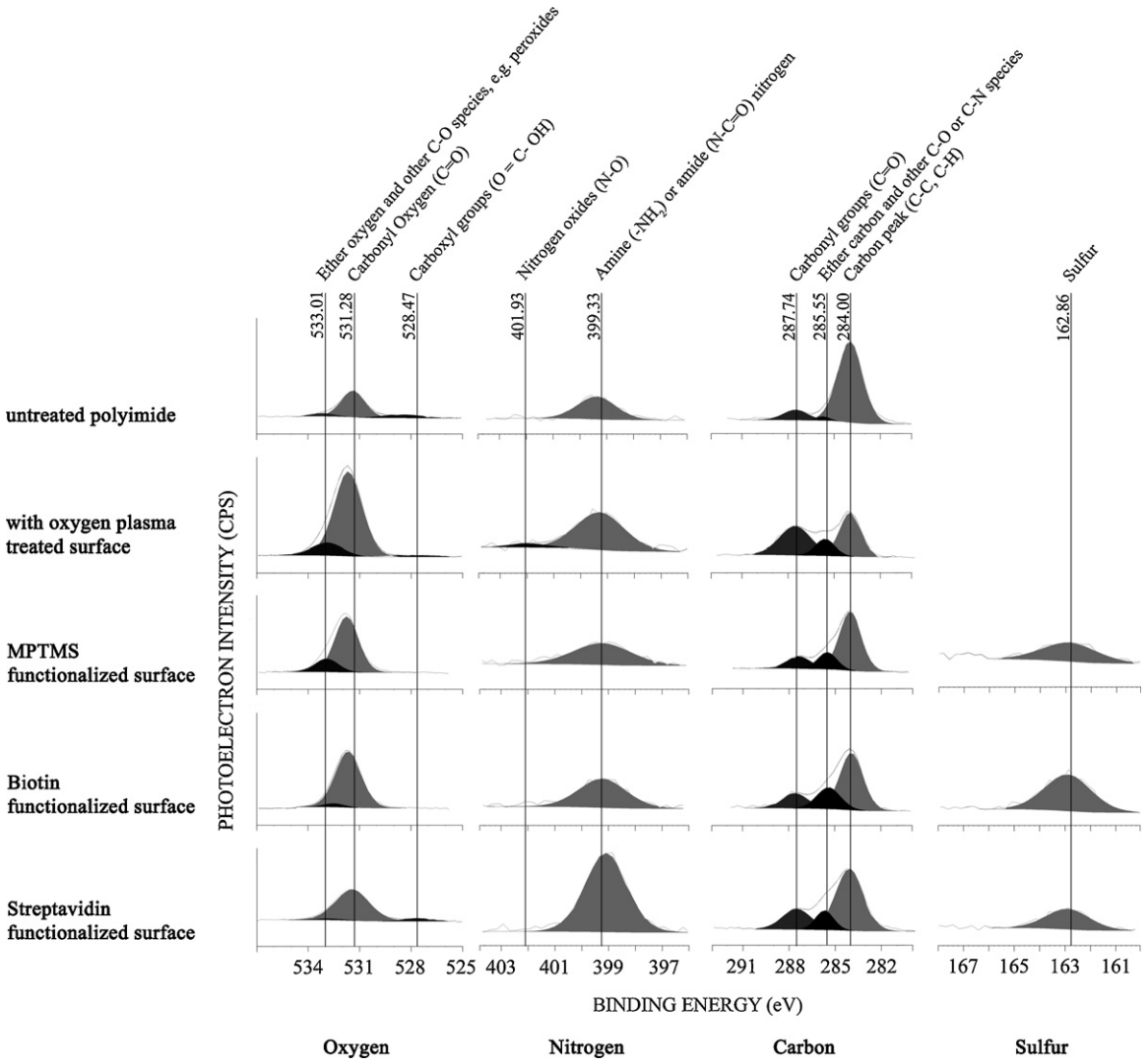

Fig. 4. Deconvoluted XPS-spectra of the relevant peaks before and after the different functionalization steps and after streptavidin immobilization.

(e.g. peak at 287.7 eV), while the C–O species increase (peak at 285.6 eV). These alterations in the XPS spectra stem from the reaction of MPTMS with surface bound oxygens. In this reaction reactive oxygen groups (e.g. C–O–H) react with alkoxysilanes of MPTMS by a condensation reaction forming a stable C–O–Si bond leading to covalent attachment to the surface. The change in the oxygen peaks, especially the fact that the carboxyl group peak vanishes after MPTMS functionalization, reveal that the carboxyl groups completely react with the MPTMS. MPTMS carries one sulfur atom, its binding to the surface introduces a sulfur peak in the XPS spectrum which was not present before (see Fig. 4). From the integral, a relative sulfur concentration of 1.15% of all detected atoms on the surface can be calculated (see Fig. 5).

Like MPTMS, also M-PEG_2-biotin has incorporated one sulfur atom per molecule. Therefore, the concentration of sulfur on the surface should again increase with the biotinylation. In the case of a 100% reaction between the maleimide groups of M-PEG_2-biotin with the thiol functional groups of the thiol-modified surface the sulfur concentration is expected to be twice as high as on the MPTMS functionalized sample. In our measurements the sulfur concentration was 1.8 times higher than by the MPTMS functionalized sample (Fig. 5), indicating a reaction rate of approximately 80%.

The XPS spectrum after the immobilization of Chromeon 642-streptavidin is mainly characterized by significant increases of nitrogen (amine/amide peak at 399.3 eV) and carbon on the surface (see Figs. 4 and 5). The deconvoluted spectra indicate that the introduced nitrogen is coming from the amide backbone and the amino groups of the protein. Moreover, the relative intensity of the carbonyl band (at 287.7 eV) is increased compared to C–O and C–<!– no-mfc –>C/C<!– /no-mfc –>–H species due to the peptide bonds in the immobilized protein (Fig. 4). It is also striking that the peak for carboxyl groups (528.5 eV), as may be expected for a protein, can be found in the spectra again. This indicates that the binding of streptavidin to the surface was successful and supported the results from the fluorescence measurements.

3.7. Measurements with polyimide based Mach-Zehnder interferometers

The described optimized functionalization procedure showed its potential for surface modification without inflicted damage to thin polyimide waveguide layers. Next, it was utilized to chemically modify the polyimide surface in the measurement window of Mach-Zehnder interferometer sensors in order to examine its functionality in MZI sensing experiments.

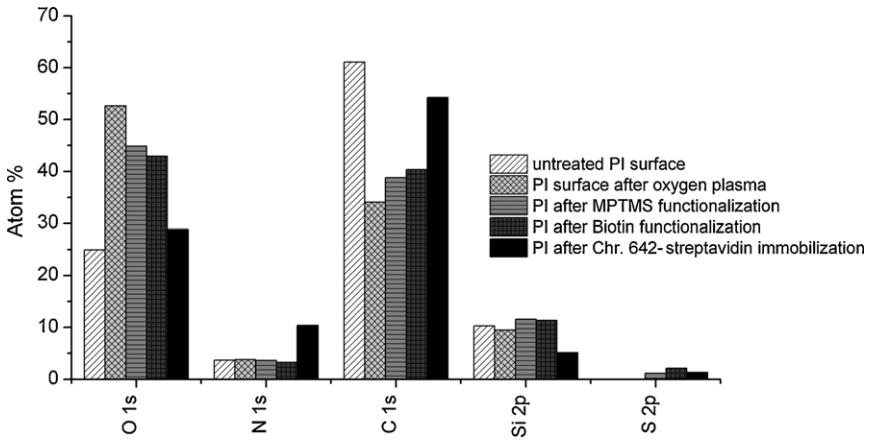

Fig. 5. Atom composition of the polyimide surfaces before and after the functionalization steps and the immobilization of streptavidin.

For the measurements the biotinylated polyimide based MZI sensors were mounted onto the measurement setup with a fluidic system on top of the sensors. First, 150 mM PBS buffer was rinsed over the sensor surface. Then, the buffer solution was exchanged against 150 mM PBS buffer containing a specific concentration of a biomolecule, such as Chromeon 642-streptavidin or unlabelled streptavidin. After the measurement the sensor surface was again rinsed with 150 mM PBS buffer in order to wash away unbound molecules from the sensor surface. The flow rate was kept constant at 20 μl min^{-1} and the measurements were carried out at a temperature of about 22 °C.

The first measurements were performed with different concentrations of Chromeon 642-streptavidin dissolved in 150 mM PBS buffer, in order to monitor the concentration dependency and to allow control fluorescence scans after the real-time MZI sensor measurements. Fig. 6 shows the phase shift that is induced in the interferometer as function of time during the measurements of different concentrations of Chromeon 642-streptavidin in ranges between 0.1 and 50 μg mL^{-1} (1.6–833 nM) on biotinylated sensor surfaces. Mechanical drifts may lead to a misalignment of the optical fibers, thus influencing the measured transmission, and subsequently, the calculated phase shift. A correction of the misalignment was thus occasionally performed by intentionally activating the auto alignment system. This process can lead to steps in the measurement curves in Fig. 6 (e.g. curves of 2.0 μg mL^{-1} at approximately 650 s and 2000 s). The parasitic effect caused by this mechanical drift can be reduced by using coupling methods that provide relaxed alignment tolerances, such as grating couplers. At low concentrations Chromeon 642-streptavidin binds slowly to the biotinylated surface inducing a weak phase shift only. The higher the concentration, the stronger the phase shifts. With the highest applied concentration of 50 μg mL^{-1} saturation of the surface occurs after around 500 s. These measurements clearly show concentration dependency of the sensor signal, as expected, and thus its principal functionality. This could also be confirmed by control fluorescence scans.

The measurements on BSA blocked biotinylated sensor surfaces showed similar results in the concentration dependency, but lead to 40% reduced signals and to a maximum phase shift of about 3.5π for 50 μg mL^{-1} [34].

While this sensing application nicely showed the functionality of surface modification and MZI sensor, respectively, detection of streptavidin was not the primary focus. In a further step, sensor surfaces for DNA hybridization were to be developed. For this purpose, streptavidin immobilized to the biotinylated sensor surface was utilized to bind biotinylated single-stranded DNA (ssDNA) to free biotin-binding sites of the tetrameric protein.

In order to prepare a high density streptavidin layer on the surface for DNA hybridization experiments, 200 μg mL^{-1} (~330 nM) of unlabelled streptavidin was dissolved in 150 mM PBS buffer and rinsed over the surface by means of the fluidic system on top of the sample. The monitoring of the binding between the unlabelled streptavidin and the biotin on the sensor surface revealed an induced phase shift of approximately 4π within 120 s before the signal remained stable. This result indicates a fast saturation of the biotinylated sensor surface with unlabelled streptavidin. The phase shift of 4π is comparable to the maximal phase shift of Chromeon 642-streptavidin (3.5π) reached on BSA blocked biotinylated sensor surfaces and lower than the maximal phase shift of Chromeon 642-streptavidin (7.5π) on unblocked sensor surfaces. This indicates a reduced unspecific interaction of the unlabelled streptavidin with the unblocked biotinylated sensor surface.

After binding of streptavidin on the surface, the samples were rinsed with PBS buffer.

The streptavidin layer on the sensor surface offers a sufficient number of binding sites for biotin. This biotin binding sites were used to perform different DNA experiments with ssDNA (see Fig. 7). The concentration of the ssDNA was kept constant at 1 μM in the following measurement series. For every DNA experiment a new biotinylated polyimide base MZI sensor was used, which was satu-

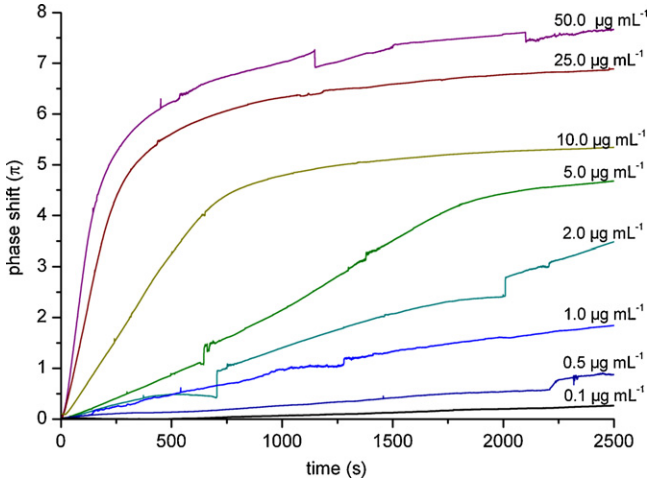

Fig. 6. Phase shifts induced in unblocked, biotinylated polyimide based Mach-Zehnder interferometers during measurements of different concentrations of Chromeon 642-streptavidin. The peaks in the curve e.g. of 2.0 μg mL^{-1} at approximately 650 s and 2000 s are caused by tracking of the optical fibers.

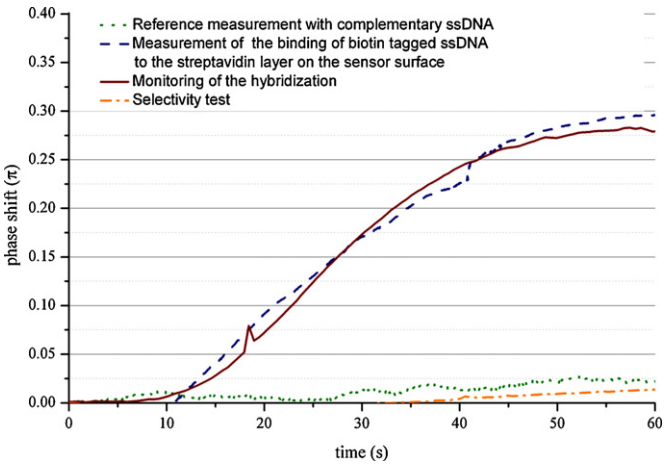

Fig. 7. Phase shifts in polyimide based MZIs during DNA experiments.

rated in the first step with unlabelled streptavidin and then rinsed with PBS buffer.

The first DNA experiment performed on the streptavidin layered MZI sensor was a reference measurement, in which complementary ssDNA was rinsed over the surface in order to test for unspecific interactions of the ssDNA with the sensor surface. In this case, no significant phase shift and therefore no non-specific interaction of the complementary ssDNA with the sensor surface could be found. In the next DNA experiment the biotin-tagged ssDNA was rinsed over the surface and a phase shift of 0.3π arising from the binding process of the biotin tag to the streptavidin layer was observed (see Fig. 7). After the immobilization of the biotin-tagged ssDNA the sensor surface was again rinsed with PBS buffer and then complementary ssDNA was flowed over the sensor surface. A phase shift of 0.27π was induced, which indicates hybridization between the complementary ssDNA. Finally, the selectivity of the hybridization was tested. For this purpose, the biotin-tagged ssDNA was first immobilized on the streptavidin layered MZI sensor surface and, after a rinsing step with PBS buffer, non-complementary ssDNA was rinsed over the surface. In this experiment, no significant phase shift, and therefore, no unspecific binding of the non-complementary DNA strands was detected (see Fig. 7). It is evident that a fully functional DNA sensor can be obtained employing the proposed surface chemistry and MZI sensor configuration.

4. Conclusion

In this work the chemical modification of polyimide films for streptavidin binding was presented. The main goal was the optimization of the surface modification procedures which consisted of oxygen plasma activation of the polyimide film, silanization with 3-mercaptopropyl trimethoxysilane, covalent attachment of maleimide-PEG_2-biotin and finally non-covalent binding of streptavidin. With fluorescent labelled Chromeon 642-streptavidin a maximum population density of 144 fmol mm^{-2} was measured on the polyimide surface by fluorescence scans. Considering the multiplicity of steps in the functionalization protocol, the reproducibility over all steps was quite satisfactory (13.9% RSD, $n = 10$). AFM measurements indicated that the thin layer polyimide gets neither damaged nor thinned and that the surface roughness stays below a mean roughness, R_a, of 0.60 nm. XPS measurements provided further information on how the functionalization with MPTMS on the oxygen plasma activated polyimide takes place and gives insight into the relative atom composition of the polyimide surface before and after the functionalization steps. The developed protocol creates a modified polyimide surface with high binding capacity for streptavidin while keeping the polyimide surface intact. This surface modification was used for the functionalization of polyimide based MZI sensors and concentrations of Chromeon 642-streptavidin with concentrations as low as 0.1 $\mu g\,mL^{-1}$ were successfully detected. Unlabelled streptavidin showed a similar binding behavior to the biotinylated sensor surface as Chromeon 642-streptavidin. In the next step, unlabelled streptavidin was used to create a high density streptavidin layer on the sensor surface as platform for advanced biosensing experiments. The streptavidin-modified polyimide based MZI sensors were used in different DNA experiments, which showed a selective binding of biotin tagged ssDNA to the surface and a selective and specific hybridization between the complementary strands.

In this work, we prove the usability of the high index polymer polyimide as wave guiding layer in evanescent wave biosensors. In medical applications, this low cost, single use disposable device can be of great benefit for the screening on relevant biomolecules and for the detection of kinetic parameters. While a multiple use of polymer evanescent wave biosensors is, in principle, possible if a regeneration protocol for the biosensitive layer can be found, our target application are single use sensor devices, which are, due to hygienic standards, preferred in many medical scenarios.

Acknowledgements

This work was supported by the Austrian NANO Initiative under the grants PLATON PolyWaG (project no. 1152) and PolyIMPD (project no. 819659). The authors want to thank DI Dr. Stephan Abermann and Dr. Ole Bethge for the support with XPS measurements, and Mag. Siegfried Krainer, Mag. Michael Stierschneider as well as Dr. Nadezhda Kataeva for the support of the surface analysis.

References

[1] K. De Vos, I. Bartolozzi, E. Schacht, P. Bienstman, R. Baets, Opt. Express 15 (2007) 7610–7615.
[2] R. Waldhäusl, B. Schnabel, P. Dannberg, E. Kley, A. Bräuer, W. Karthe, Appl. Opt. 36 (1997) 9383–9390.
[3] R.G. Heideman, R.P.H. Kooyman, J. Greve, Sens. Actuators. B Chem. 10 (1993) 209–217.
[4] B. Schneider, E.L. Dickinson, M.D. Vach, Biosens. Bioelectron. 15 (2000) 13–22.
[5] S. Busse, M. DePaoli, G. Wenz, Sens. Actuators 80 (2001) 116–124.
[6] L.M. Lechuga, A. Lenferink, R. Kooyman, Sens. Actuators B 25 (1995) 762–765.
[7] E.F. Schipper, S. Rauchalles, R. Kooyman, B. Hock, J. Greve, Anal. Chem. 70 (1998) 1192–1197.
[8] K. Tiefenthaler, W. Lukosz, J. Opt. Soc. Am. B 6 (1989) 209–220.
[9] O. Parriaux, G.J. Veldhuis, IEEE J. Lightwave Technol. 16 (1998) 573–582.
[10] A. Densmore, D.X. Xu, S. Janz, P. Waldron, T. Mischki, G. Lopinski, A. Delâge, J. Lapointe, P. Cheben, B. Lamontagne, J.H. Schmid, Opt. Lett. 33 (2008) 596–598.
[11] K. Zinoviev, L.G. Carrascosa, J. Sanchez del Rio, B. Sepulveda, C. Dominguez, L.M. Lechuga, Adv. Opt. Technol. (2008) (Article ID 383927).
[12] R. Bruck, R. Hainberger, Proc. SPIE (7138) (2008) 71380N.
[13] N.M. Green, Adv. Protein Chem. 29 (1975) 85–133.
[14] N. Barie, M. Rapp, H. Sigrist, H.J. Ache, Biosens. Bioelectron. 13 (1998), 885-860.
[15] T. Verdianz, H. Simbürger, R. Liska, Eur. Polym. J. 42 (2006) 638–654.
[16] L. Ying Jiang, T. Shung Chung, J. Membr. Sci. 346 (2010) 45–58.
[17] R.R. Thomas, L.S. Buchwalter, L.P. Buchwalter, T.H. Chao, Macromolecules 25 (1995) 4559–4568.
[18] X.D. Huang, S.M. Bhangale, P.M. Moran, N.L. Yakovlev, J. Pan, Polym. Int. 52 (2003) 1064–1069.
[19] H.J. Kim, Y.J. Park, J. Choi, H.S. Han, Y.T. Hong, J. Ind. Eng. Chem. 15 (2009) 23–30.
[20] H.J. Leary, D.S. Campbell, Polym. Sci. Technol. 29 (1984) 517–523.
[21] M. Ali, B. Schiedt, K. Healy, R. Neumann, W. Ensinger, Nanotechnology 19 (085713) (2008) 6 pp.
[22] Z. Wei, L. Weiping, L. Huicong, Z. Liqun, Chin. J. Aeronaut. 23 (2010) 268–273.
[23] B. Zhu, H. Iwata, I. Hirata, Y. Ikada, J. Adhes. Sci. Technol. 14 (2000) 351–361.
[24] R. Flitsch, Y. Shih, J. Vac. Sci. Technol. A 8 (1990) 2379–2381.
[25] Y. Nakamura, Y. Suzuki, Y. Watanabe, Thin Solid Films 290–291 (1996) 367–369.
[26] D.X. Xu, A. Densmore, A. Delâge, Opt. Express 16 (2008) 1517–15148.
[27] S. Busse, V. Scheumann, B. Menges, S. Mittler, Biosens. Bioelectron. 17 (2002) 704–710.
[28] M. Iqbal, M. Gleeson, B. Spaugh, F. Tybor, W. Gunn, M. Hochberg, T. Baehr-Jones, R. Bailey, L.C. Gunn, IEEE J. Selected Topics Quantum Electron. 16 (2010) 654–661.

[29] B. Preinerstorfer, D. Lubda, W. Lindner, M. Lämmerhofer, J. Chromatogr. A 1106 (2006) 94–105.
[30] G.T. Hermanson, Bioconjugate Techniques, Second ed., Elsevier, London, 2008, 2008.
[31] J. Spinke, M. Liley, F.J. Schmitt, J. Chem. Phys. 99 (1993) 7012–7019.
[32] S.A. Darst, M. Ahlers, P.H. Meller, Biophys. J. Biophys. Soc. 59 (1991) 387–396.
[33] F. Pippig, A. Holländer, Macromol. Biosci. 10 (2010) 1093–1105.
[34] R. Bruck, E. Melnik, P. Muellner, R. Hainberger, M. Lämmerhofer, Biosens. Bioelectron. 26 (2011) 3832–3837.